


 Cite this: *Chem. Commun.*, 2019, 55, 13896

 Received 15th July 2019,
 Accepted 25th October 2019

DOI: 10.1039/c9cc05438c

rsc.li/chemcomm

A dithiocarbamate-based H₂O₂-responsive prodrug for combinational chemotherapy and oxidative stress amplification therapy†

 Qingqing Pan,^a Boya Zhang,^a Xinyu Peng,^a Shiyu Wan,^b Kui Luo,^c Wenxia Gao,^d Yuji Pu^d*^a and Bin He^a

Here, we report the rational design of a H₂O₂-responsive diethyl-dithiocarbamate (DTC)-based prodrug, which chelated Cu(II) to form Cu(DTC)₂ with a high anticancer activity in a tumor-microenvironment and induced oxidative stress amplification, showing superior anti-tumor toxicity to disulfiram.

Disulfiram (DSF) is an oral aldehyde dehydrogenase (ALDH) inhibitor and has been approved by the FDA in the treatment of alcoholism.¹ Recently, its excellent *in vitro* anticancer activity has garnered wide attention and it has been explored as a candidate for drug repurposing in cancer therapy.^{2,3} It is mainly metabolized to diethyldithiocarbamate (DTC), which could form a complex with Cu(II) to give cancericidal Cu(DTC)₂ (Scheme S1, ESI†).^{4–7} Although DSF exhibits a broad anticancer activity, its clinical translation is still severely hindered by its super-instability both in the acidic gastric environment and in the bloodstream, compromising the *in vivo* antitumor efficacy through degradation into metabolites without anticancer activity.⁸ To address the stability issue of DSF, polymer-based drug delivery systems (DDSs) have been exploited to physically load DSF, avoiding the direct contact with blood and prolonging the half-life of DSF.^{9–12} However, the inefficient DSF loading (drug loading contents of DSF are about 2–5%) and potential drug leakage during drug delivery inevitably limit their further clinical translation. Recently, Cu(DTC)₂, rather than DSF, has been directly encapsulated into DDSs for enhanced anticancer effect.^{13–16} However, Cu(DTC)₂ lacks the selective inhibition ability between cancerous and healthy cells.

A prodrug is an effective strategy to improve DSF's bioavailability and avoid the limitations such as poor stability and tumor selectivity. For example, tumor-microenvironment-sensitive prodrugs could significantly enhance the tumor selectivity *via* stimuli-responsive drug release in tumor tissues.¹⁷ Reactive oxygen species (ROS) are abundant in various tumors and have been utilized as an endogenous stimulus to construct smart ROS-responsive prodrugs and DDSs.^{18–21} ROS can promote cell proliferation and differentiation at low concentration yet induce apoptosis at high concentration. Because of the elevated ROS level, cancer cells are under oxidative stress and are more susceptible to additional ROS invasion; they adapt to oxidative stress by upregulating antioxidant systems (such as glutathione, GSH) to maintain the ROS homeostasis. Therefore, a prodrug or DDS that can trigger both ROS generation and inhibition of the ROS-scavenging system can amplify the intracellular oxidative stress for efficient cancer cell inhibition, fulfilling an oxidative stress amplification therapy.^{22–26}

Herein, we developed a H₂O₂-responsive prodrug DQ (Fig. 1A) that could release DTC and quinone methide (QM) in the presence of H₂O₂, which is an important type of ROS present in high concentrations in tumor tissues (50–100 μM). Aryl boronic esters were used as H₂O₂-responsive moieties owing to the ease of synthesis and good biocompatibility.^{27–29} DQ was cleaved by H₂O₂ to release DTC by a B–C bond-cleavage and a following 1,6-benzyl elimination.^{30–32} The DTC chelated Cu(II) to generate Cu(DTC)₂ with high anticancer activity. The chelation process, like the reaction of DSF and Cu(II), could induce the elevation of intracellular ROS.^{7,8} In addition, the released QM exerted as a GSH-scavenging agent to inhibit the GSH-mediated ROS elimination in cancer cells.^{33,34} The simultaneous ROS generation and GSH depletion cooperated collectively to amplify oxidative stress and killed cancer cells through apoptosis (Fig. 1B). The DQ prodrug was demonstrated to be effective for *in vitro* and *in vivo* cancer cell inhibition by a combination of Cu(DTC)₂-based chemotherapy and oxidative stress amplification.

The prodrug DQ was synthesized by facile reaction of sodium diethylthiocarbamate and 4-bromomethylphenylboronic acid

^a National Engineering Research Center for Biomaterials, Sichuan University, Chengdu 610064, China. E-mail: yjpu@scu.edu.cn

^b School of Chemical Engineering, Sichuan University, Chengdu 610065, China

^c Huaxi MR Research Center (HMRRC), Department of Radiology, West China Hospital, Sichuan University, Chengdu 610041, China

^d College of Chemistry & Materials Engineering, Wenzhou University, Wenzhou 325027, China

† Electronic supplementary information (ESI) available: Synthesis and characterization of prodrug DQ. ROS-responsiveness results of DQ and the *in vitro* and *in vivo* biological results. See DOI: 10.1039/c9cc05438c

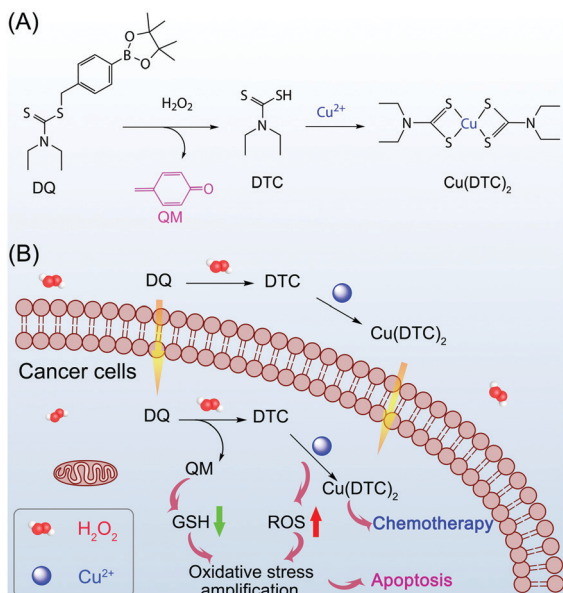


Fig. 1 (A) The proposed H_2O_2 -responsive mechanism of DQ prodrug to release QM and DTC. DTC chelates the available $\text{Cu}(\text{II})$ to give the anticancer drug $\text{Cu}(\text{DTC})_2$. (B) The therapeutic process of the DQ prodrug for combinational chemotherapy and oxidative stress amplification therapy.

pinacol ester in a mixed solvent of methanol and tetrahydrofuran (Scheme S2, ESI[†]). The chemical structure of DQ was verified by ^1H and ^{13}C NMR and ESI-MS (Fig. S2–S4, ESI[†]).

The H_2O_2 -responsiveness of DQ was first investigated by ^1H NMR (Fig. 2A and Fig. S5, ESI[†]). The ^1H NMR spectra of DQ after the treatment of H_2O_2 for different times were obtained using a mixed solvent of $\text{DMSO}-d_6/\text{D}_2\text{O}$ (v/v, 9:1). Consistent with the previous NMR study of benzyl boronic ester-cleavage in response to H_2O_2 ,³⁵ new peaks of 4-hydroxybenzyl alcohol, which was the addition product of water to QM, were observed at 6.7 and 7.2 ppm; the peaks at 7.4 and 7.7 ppm were ascribed to the partly hydrolytic product of boronic acid. Kinetics study revealed that the reaction was a pseudo-first order reaction with a half-life of 1.33 h (Fig. S6, ESI[†]), indicating that DTC could be rapidly released relative to persulfides (7.5 h).³⁵ In contrast, no obvious cleavage of DQ was observed in the absence of H_2O_2 after 7 h and around 28% hydrolysis was observed after 48 h (Fig. 2B and Fig. S7, ESI[†]), demonstrating the slow degradation of DQ in the absence of H_2O_2 . Importantly, there was no generation of 4-hydroxybenzyl alcohol in the hydrolysis, suggesting no release of DTC by mere hydrolysis and thus presumably displaying low systemic toxicity in a further *in vivo* study.

To further confirm the H_2O_2 -responsive release of DTC and the formation of $\text{Cu}(\text{DTC})_2$ in the presence of $\text{Cu}(\text{II})$, we performed a fluorescence competition assay.^{17,36} As shown in Fig. 2C, the fluorescence of calcein was quenched by $\text{Cu}(\text{II})$ binding. Instant fluorescence recovery was observed after the addition of excessive DTC in the DTC group, demonstrating the rapid chelation between DTC and $\text{Cu}(\text{II})$. The DQ group showed time-dependent fluorescence recovery, suggesting the H_2O_2 -triggered sustained release of DTC. As shown in the dynamic light scattering results

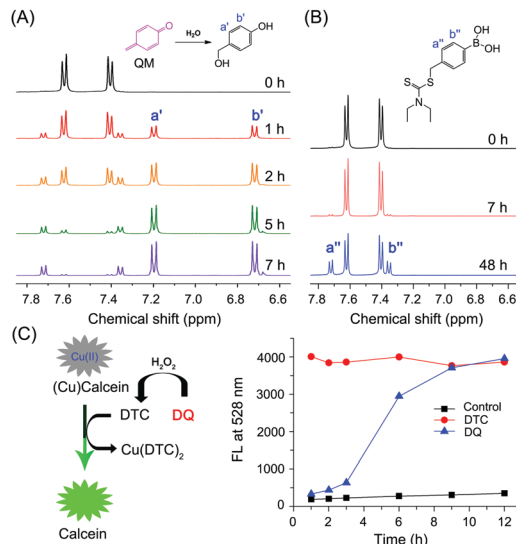


Fig. 2 ^1H NMR spectra changes of DQ in the presence (A) and absence (B) of H_2O_2 . (C) The illustration of the fluorescence competition assay and the fluorescence changes over time.

(Fig. S8, ESI[†]), high concentration of DQ ($12.5 \mu\text{M}$) formed nanoparticles in aqueous solution ($\text{DMSO}/\text{H}_2\text{O} = 0.05\%/99.95\%$, v/v). The nanoparticles limited sufficient contact between H_2O_2 and DQ molecules and thus the fluorescence recovery was slow in the beginning. The formation of $\text{Cu}(\text{DTC})_2$ in the fluorescence competition assay was further demonstrated by analyzing the mixtures at 12 h *via* ESI-MS (Fig. S9, ESI[†]).¹⁷ Together, these results validated that DQ could be activated by H_2O_2 to release DTC, which could chelate with available $\text{Cu}(\text{II})$ to generate $\text{Cu}(\text{DTC})_2$.

We studied the cytocompatibility of DQ using DSF as a control. NIH 3T3 cells were incubated with DQ or DSF at varying concentrations for 24 h; the cell viability was then tested by an MTT assay (Fig. 3A). DQ showed a much lower cytotoxicity ($\text{IC}_{50} > 100 \mu\text{M}$) to normal cells than DSF (IC_{50} of $12.5 \mu\text{M}$). We also investigated the anticancer activity of DSF and DQ against 4T1 cancer cells in the presence and absence of $\text{Cu}(\text{II})$. DSF or DQ alone showed low cytotoxicity to 4T1 cancer cells (Fig. 3B). However, additional extracellular $\text{Cu}(\text{II})$ ($1 \mu\text{M}$)¹⁷ significantly enhanced their anticancer activity; the IC_{50} values of DQ and DSF in the condition of $1 \mu\text{M}$ $\text{Cu}(\text{II})$ were 0.33 and $1.4 \mu\text{M}$,

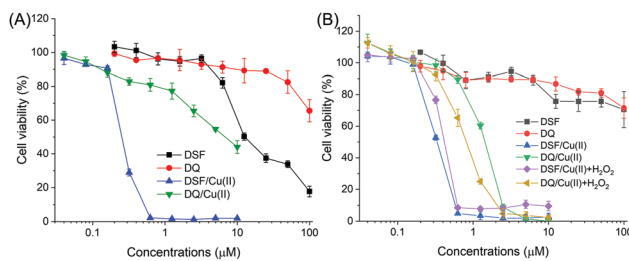


Fig. 3 The cell viabilities of NIH 3T3 (A) and 4T1 (B) cells after being treated with DSF and DQ at different concentrations. The concentrations of H_2O_2 and $\text{Cu}(\text{II})$ were 10 and $1 \mu\text{M}$, respectively.

respectively (Fig. 3B). DSF showed a similar cytotoxicity to NIH 3T3 cells (IC_{50} : $0.25 \mu\text{M}$) in the presence of $\text{Cu}(\text{II})$ (Fig. 3A). However, DQ could induce much less cytotoxicity to NIH 3T3 cells (IC_{50} : $6.58 \mu\text{M}$), suggesting higher selectivity to inhibit cancer cells.

We then studied whether H_2O_2 plus $\text{Cu}(\text{II})$ could enhance the anticancer activity of DQ in 4T1 cells. Exogenous H_2O_2 was supplemented because the H_2O_2 concentration of *in vitro* cancer cells was much lower than that of tumor tissue and the cell culture medium could consume H_2O_2 . We explored the appropriate H_2O_2 concentration for *in vitro* study by an MTT assay (Fig. S10, ESI[†]); the extracellular H_2O_2 concentration in this study was set to be $10 \mu\text{M}$. As shown in Fig. 3B, H_2O_2 showed negligible effect on the anticancer activity of DSF (IC_{50} : $0.40 \mu\text{M}$). In contrast, DQ showed significantly enhanced anticancer efficacy (IC_{50} : $0.80 \mu\text{M}$) with the assistance of H_2O_2 and $\text{Cu}(\text{II})$. Given that DSF was a dimer of DTC, from the point of DTC amounts in DSF and DQ, DQ showed comparable *in vitro* anticancer efficiency to DSF in the presence of H_2O_2 and $\text{Cu}(\text{II})$.

To explore whether DQ could induce oxidative stress amplification in the presence of H_2O_2 and $\text{Cu}(\text{II})$, we studied the intracellular ROS level in 4T1 cells by flow cytometry and confocal laser scanning microscopy (CLSM) using DCFH as a probe (Fig. 4A and B). $\text{H}_2\text{O}_2 + \text{Cu}(\text{II})$ treated cells were used as a control. A H_2O_2 -consuming benzyl boronic ester without DTC-producing ability (**B**, the structure was shown in the inset in the Fig. 4A) was used as a negative control. Cells treated with $1 \mu\text{M}$ **B** showed a lower intracellular ROS level than the control group, confirming the H_2O_2 -consuming capability. In stark contrast, cells treated with $1 \mu\text{M}$ DSF and DQ showed comparable, significantly elevated ROS level, which was ascribed to the formation of $\text{Cu}(\text{DTC})_2$. A higher concentration of DQ ($2 \mu\text{M}$, equivalent to $1 \mu\text{M}$ DSF) further elevated the intracellular ROS level. CLSM results further confirmed the intracellular ROS

results (Fig. 4B). Thereafter, the intracellular GSH contents were studied by a GSH–GSSG method. DSF induced negligible GSH reduction. However, 1 and $2 \mu\text{M}$ DQ treatment resulted in a remarkable reduction of the GSH contents of 13.0% and 19.6% , respectively (Fig. 4C), verifying the GSH-depletion property of QM. Taking together, DQ can be activated by H_2O_2 and incur oxidative stress amplification of 4T1 cells.

Since apoptosis is the main way of cancer cell death when cells suffer from elevated oxidative level, we then performed a cell apoptosis study to confirm the oxidative stress amplification. As shown in Fig. 4D and Fig. S12 (ESI[†]), both DSF and DQ caused remarkably enhanced apoptosis (total apoptosis of $\sim 60\%$ when cells were treated with $1 \mu\text{M}$ DSF and $2 \mu\text{M}$ DQ) relative to the H_2O_2 and $\text{Cu}(\text{II})$ treated group (control group). $\text{Cu}(\text{DTC})_2$ showed comparable cell apoptosis to the control group, confirming its anticancer mechanism in a non-apoptosis manner.^{14,16} A new compound QAc (chemical structure and NMR result were shown in Fig. S11, ESI[†]), which can be activated by H_2O_2 to release QM, was synthesized as a negative control and showed a slight increase of cell apoptosis rate. Collectively, we confirmed that DQ could induce high apoptosis rate of 4T1 cells. Although DSF had a negligible effect in GSH consumption, it still induced high cell apoptosis because of the prompt reaction of DSF and $\text{Cu}(\text{II})$ and their interactions with cancer cells.

The stability of DQ and DSF in blood was then studied by monitoring their concentrations in mice blood after intravenous administration. The blood concentrations of DQ were 5-fold higher than those of DSF in the first 4 h (Fig. S13, ESI[†]), suggesting the superior biostability of DQ.

Encouraged by the excellent *in vitro* anticancer activity and enhanced *in vivo* stability of DQ, we further evaluated the *in vivo* anticancer efficacy in the 4T1 tumor-bearing female Balb/C mice. Copper(II) gluconate (CuGlu) was supplemented orally at a dose of 1.5 mg kg^{-1} in all $\text{Cu}(\text{II})$ -involved groups. DSF was intravenously injected with a dose of 15 mg kg^{-1} . DQ was administrated similarly with two different doses (18.5 and 37 mg kg^{-1} in the $\text{DQ}/\text{Cu}(\text{II})$ and $\text{DQ} \times 2/\text{Cu}(\text{II})$ groups, which were respectively half and the same equivalent amount of DTC to 15 mg kg^{-1} DSF). The body weights of tumor-bearing mice were monitored to study the systemic toxicity (Fig. 5A). All the groups showed a similar trend to the saline group, indicating the low systemic toxicity of DSF and DQ. The tumor volumes were monitored and the results are shown in Fig. 5B. The tumor volumes of the CuGlu group were close to those of the saline group, manifesting that CuGlu alone had no therapeutic effect. The $\text{DQ} \times 2/\text{Cu}(\text{II})$ group showed the best antitumor efficacy and the $\text{DQ}/\text{Cu}(\text{II})$ group showed slightly enhanced anticancer effect towards the $\text{DSF}/\text{Cu}(\text{II})$ group. The tumor inhibition rates of the $\text{DSF}/\text{Cu}(\text{II})$, $\text{DQ}/\text{Cu}(\text{II})$, and $\text{DQ} \times 2/\text{Cu}(\text{II})$ groups were 48.1% , 57.5% , and 78.3% , respectively (Fig. S14, ESI[†]).

Histological analysis was further carried out to assess the organ toxicity by H&E staining. The cell necrosis in the $\text{DQ} \times 2/\text{Cu}(\text{II})$ group was more serious than that in the $\text{DSF}/\text{Cu}(\text{II})$ and $\text{DQ}/\text{Cu}(\text{II})$ groups (Fig. 5C). Moreover, low toxicity to normal organs was observed in these groups (Fig. S15, ESI[†]), suggesting the relatively low organ toxicity of DSF and DQ.

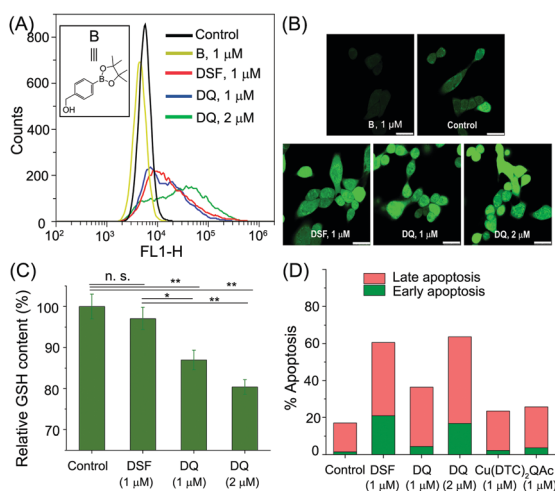


Fig. 4 The intracellular ROS levels of 4T1 cells, determined by flow cytometry (A) and CLSM (B), after being treated with different formulations. Relative intracellular GSH contents (C) and cell apoptosis percentages (D) of 4T1 cells treated with different formulations. (n.s., not significant; *, $p < 0.05$; and **, $p < 0.01$, $n = 3$.)

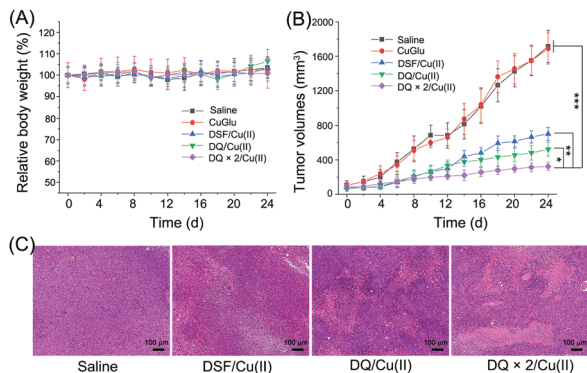


Fig. 5 The body weights (A) and tumor volumes (B), and H&E staining images (C) of tumor-bearing mice treated with saline, CuGlu, DSF/Cu(II), DQ/Cu(II), and DQ \times 2/Cu(II). ($n = 5$, *, $p < 0.05$; **, $p < 0.01$, ***, $p < 0.001$.) (C) H&E stained images of tumor slices taken from different groups at day 24.

In summary, we have reported a DTC-based prodrug for combinational chemotherapy and oxidative stress amplification therapy. High concentrations of H_2O_2 and copper are beneficial for prodrug activation to release DTC and GSH consuming QM.^{18,37,38} The ROS-responsive prodrug DQ with copper-dependent cytotoxicity realized tumor-specific toxicity with low toxicity to normal organs. Our study provides a new delivery strategy of DSF and metal-based anticancer drugs.

This work was supported by the National Natural Science Foundation of China (No. 51773130 and 51573111), Fundamental Research Funds for the Central Universities (YJ201764), Sichuan Science and Technology Program (2019YJ0051), and Jiangsu International Cooperation project (BZ2017062). We would like to thank the Analytical & Testing Center of Sichuan University for NMR spectroscopy.

Conflicts of interest

There are no conflicts to declare.

Notes and references

- 1 R. Vallari and R. Pietruszko, *Science*, 1982, **216**, 637–639.
- 2 D. Chen, Q. C. Cui, H. Yang and Q. P. Dou, *Cancer Res.*, 2006, **66**, 10425–10433.
- 3 K. Iljin, K. Ketola, P. Vainio, P. Halonen, P. Kohonen, V. Fey, R. C. Grafström, M. Perälä and O. Kallioniemi, *Clin. Cancer Res.*, 2009, **15**, 6070–6078.
- 4 Z. Skrott, M. Mistrik and K. K. Andersen, *et al.*, *Nature*, 2017, **552**, 194–199.
- 5 D. Cen, D. Brayton, B. Shahandeh, F. L. Meyskens and P. J. Farmer, *J. Med. Chem.*, 2004, **47**, 6914–6920.
- 6 D. J. Lewis, P. Deshmukh, A. A. Tedstone, F. Tuna and P. O'Brien, *Chem. Commun.*, 2014, **50**, 13334–13337.

- 7 P. E. Tawari, Z. Wang, M. Najlah, C. W. Tsang, V. Kannappan, P. Liu, C. McConville, B. He, A. L. Armesilla and W. Wang, *Toxicol. Res.*, 2015, **4**, 1439–1442.
- 8 K. Butcher, V. Kannappan, R. S. Kilari, M. R. Morris, C. McConville, A. L. Armesilla and W. Wang, *BMC Cancer*, 2018, **18**, 753–764.
- 9 L. Zhang, B. Tian, Y. Li, T. Lei, J. Meng, L. Yang, Y. Zhang, F. Chen, H. Zhang, H. Xu, Y. Zhang and X. Tang, *ACS Appl. Mater. Interfaces*, 2015, **7**, 25147–25161.
- 10 P. Zhao, W. Yin, A. Wu, Y. Tang, J. Wang, Z. Pan, T. Lin, M. Zhang, B. Chen, Y. Duan and Y. Huang, *Adv. Funct. Mater.*, 2017, **27**, 1700403.
- 11 X. Duan, J. Xiao, Q. Yin, Z. Zhang, H. Yu, S. Mao and Y. Li, *ACS Nano*, 2013, **7**, 5858–5869.
- 12 W. Song, Z. Tang, N. Shen, H. Yu, Y. Jia, D. Zhang, J. Jiang, C. He, H. Tian and X. Chen, *J. Controlled Release*, 2016, **231**, 94–102.
- 13 M. Wehbe, M. Anantha, M. Shi, A. W.-Y. Leung, W. H. Dragowska, L. Sanche and M. B. Bally, *Int. J. Nanomed.*, 2017, **12**, 4129–4146.
- 14 W. Chen, W. Yang, P. Chen, Y. Huang and F. Li, *ACS Appl. Mater. Interfaces*, 2018, **10**, 41118–41128.
- 15 P. Zhao, Y. Wang, X. Kang, A. Wu, W. Yin, Y. Tang, J. Wang, M. Zhang, Y. Duan and Y. Huang, *Chem. Sci.*, 2018, **9**, 2674–2689.
- 16 X. Peng, Q. Pan, B. Zhang, S. Wan, S. Li, K. Luo, Y. Pu and B. He, *Biomacromolecules*, 2019, **20**, 2372–2383.
- 17 S. Bakthavatsalam, M. L. Sleeper, A. Dharani, D. J. George, T. Zhang and K. J. Franz, *Angew. Chem., Int. Ed.*, 2018, **57**, 12780–12784.
- 18 A. Gupte and R. J. Mumper, *Cancer Treat. Rev.*, 2009, **35**, 32–46.
- 19 L. Xu, Y. Yang, M. Zhao, W. Gao, H. Zhang, S. Li, B. He and Y. Pu, *J. Mater. Chem. B*, 2018, **6**, 1076–1084.
- 20 L. Xu, M. Zhao, Y. Yang, Y. Liang, C. Sun, W. Gao, S. Li, B. He and Y. Pu, *J. Mater. Chem. B*, 2017, **5**, 9157–9164.
- 21 J. Noh, B. Kwon, E. Han, M. Park, W. Yang, W. Cho, W. Yoo, G. Khang and D. Lee, *Nat. Commun.*, 2015, **6**, 6907.
- 22 J. Li, A. Dirisala, Z. Ge, Y. Wang, W. Yin, W. Ke, K. Toh, J. Xie, Y. Matsumoto, Y. Anraku, K. Osada and K. Kataoka, *Angew. Chem.*, 2017, **129**, 14213–14218.
- 23 L. S. Lin, J. Song, L. Song, K. Ke, Y. Liu, Z. Zhou, Z. Shen, J. Li, Z. Yang, W. Tang, G. Niu, H. H. Yang and X. Chen, *Angew. Chem., Int. Ed.*, 2018, **57**, 4902–4906.
- 24 W. Zhang, J. Lu, X. Gao, P. Li, W. Zhang, Y. Ma, H. Wang and B. Tang, *Angew. Chem., Int. Ed.*, 2018, **57**, 4891–4896.
- 25 W. Yin, W. Ke, W. Chen, L. Xi, Q. Zhou, J. F. Mukerabigwi and Z. Ge, *Biomaterials*, 2019, **195**, 63–74.
- 26 Z. Dong, L. Feng, Y. Chao, Y. Hao, M. Chen, F. Gong, X. Han, R. Zhang, L. Cheng and Z. Liu, *Nano Lett.*, 2018, **19**, 805–815.
- 27 C.-C. Song, F.-S. Du and Z.-C. Li, *J. Mater. Chem. B*, 2014, **2**, 3413–3426.
- 28 Y. Xu, W. Shi, H. Li, X. Li and H. Ma, *ChemMedChem*, 2019, **14**, 1079–1085.
- 29 Y. Hu, X. Li, Y. Fang, W. Shi, X. Li, W. Chen, M. Xian and H. Ma, *Chem. Sci.*, 2019, **10**, 7690–7694.
- 30 J. L. Major Jourden and S. M. Cohen, *Angew. Chem.*, 2010, **122**, 6947–6949.
- 31 M. Ye, Y. Han, J. Tang, Y. Piao, X. Liu, Z. Zhou, J. Gao, J. Rao and Y. Shen, *Adv. Mater.*, 2017, **29**, DOI: 10.1002/adma.201702342.
- 32 Y. Han, W. Yin, J. Li, H. Zhao, Z. Zha, W. Ke, Y. Wang, C. He and Z. Ge, *J. Controlled Release*, 2018, **273**, 30–39.
- 33 H. Hagen, P. Marzenell, E. Jentsch, F. Wenz, M. R. Veldwijk and A. Mokhir, *J. Med. Chem.*, 2012, **55**, 924–934.
- 34 C. Q. Luo, Y. X. Zhou, T. J. Zhou, L. Xing, P. F. Cui, M. Sun, L. Jin, N. Lu and H. L. Jiang, *J. Controlled Release*, 2018, **274**, 56–68.
- 35 C. R. Powell, K. M. Dillon, Y. Wang, R. J. Carrarzone and J. B. Matson, *Angew. Chem., Int. Ed.*, 2018, **57**, 6324–6328.
- 36 A. Warshawsky, I. Rogachev, Y. Patil, A. Baszkin, L. Weiner and J. Gressel, *Langmuir*, 2001, **17**, 5621–5635.
- 37 D. Trachootham, J. Alexandre and P. Huang, *Nat. Rev. Drug Discovery*, 2009, **8**, 579–591.
- 38 K. G. Daniel, D. Chen, S. Orlu, Q. C. Cui, F. R. Miller and Q. P. Dou, *Breast Cancer Res.*, 2005, **7**, R897–R908.